Semi-Online Precoding with Information Parsing for Cooperative MIMO Wireless Networks

Juncheng Wang*, Ben Liang*, Min Dong†, Gary Boudreau‡, and Hatem Abou-zeid‡

*Department of Electrical and Computer Engineering, University of Toronto, Canada,

†Department of Electrical, Computer, and Software Engineering, Ontario Tech University, Canada, ‡Ericsson Canada, Canada

Abstract—We consider cooperative multiple-input multiple-output (MIMO) precoding design with multiple access points (APs) assisted by a central controller (CC) in a fading environment. Even though each AP may have its own local channel state information (CSI), due to the communication delay in the backhaul, neither the APs nor the CC has timely global CSI. Under this semi-online setting, our goal is to minimize the accumulated precoding deviation between the actual local precoders executed by the APs and an ideal cooperative precoder based on the global CSI, subject to per-AP transmit power limits. We propose an efficient algorithm, termed Semi-Online Precoding with Information Parsing (SOPIP), which accounts for the network heterogeneity in information timeliness and computational capacity. SOPIP does not require the CC to send the full global CSI to each AP. Instead, it takes advantage of the precoder structure to substantially lower the communication overhead, while allowing each AP to effectively combine its own timely local CSI with the delayed global CSI to enable adaptive precoder updates. We analyze the performance of SOPIP in the presence of both multi-slot communication delay and gradient estimation error, showing that it has a bounded performance gap from an offline optimal solution. Simulation results under typical Long-Term Evolution network settings further demonstrate the substantial performance gain of SOPIP over other centralized and distributed schemes.

I. Introduction

Multiple-input multiple-output (MIMO) and cooperative transmission have been recognized as two enabling techniques to meet the ever-increasing service demand of mobile devices [1]. In MIMO networks, each access point (AP) is equipped with multiple antennas and serves multiple mobile devices simultaneously via MIMO precoding [2]. Meanwhile, cooperative transmission enables multiple APs to jointly transmit signals to the mobile devices to mitigate interference and improve the received signal strength [3]. Different cooperation schemes have been proposed under various system architectures, *e.g.,* coordinated multi-point transmission in cellular networks [4], cloud-radio access network [5], and cell-free massive MIMO [6]. In a cooperative wireless network, it is commonly assumed that the APs are connected to a central controller (CC) via ideal backhaul. However, cooperative transmission over non-ideal backhaul with communication delay and limited capacity is a practical concern.

Cooperative precoding design intrinsically requires the knowledge of global channel state information (CSI) due to the coupling between the channels and precoders of the APs. Therefore, most prior works adopted a *global* processing approach to design cooperative precoding at the CC, assuming the global CSI is readily available [7]-[14]. Some other works considered distributed cooperative precoding design at the APs based only on the local CSI [15]-[17]. However, due to the lack of global CSI, such *local* processing approach cannot fully utilize the degrees of freedom to effectively mitigate interference. In contrast, the *joint* (global and local) processing approach utilizes the computational capacity at both the CC and the APs via information exchange between them over the backhaul, to achieve full degrees of freedom [18]-[22]. In this work, we adopt the joint processing approach.

All of the existing works that adopt the joint processing approach have focused on *offline* cooperative precoding problems assuming the CSI is known apriori. However, in practical cooperative wireless networks, non-ideal backhaul can cause severe communication delay between the CC and the APs. *Online* precoding design was considered for global processing in [23]-[25] based on delayed CSI. However, these works focused on single-cell systems and did not consider cooperative transmission. There is no existing work on online cooperative precoding design.

It is challenging to tackle the semi-online cooperative precoding problem. First, the design of cooperative precoding is intrinsically non-separable among the APs and therefore requires the knowledge of global CSI. Second, due to the non-ideal backhaul, neither the CC nor the APs has the timely global CSI to design the cooperative precoder. Third, the APs need to implement real-time local precoders while cooperating with each other to mitigate interference. Finally, we should take full advantage of both the timely local CSI at the APs and the delayed global CSI at the CC, and this calls for a *semi-online* cooperative precoding design for joint processing.

In this work, we aim at developing a semi-online algorithm to fully utilize the timely local CSI at the APs for a CC-assisted cooperative precoding solution. We formulate a precoding optimization problem to minimize the accumulated deviation between the received signals from the actual local precoders executed by the APs and any desired cooperative precoder assuming non-delayed perfect global CSI. The main contributions of this paper are as follows:

- We formulate the above problem of cooperative MIMO precoding over non-ideal backhaul as a semi-online optimization problem, where the APs have timely local CSI but require the assistance of a CC that has additional computational resource and delayed global CSI. At each time slot, each AP computes and executes its own local precoder, but all APs cooperatively minimize the accumulated deviation between the actual cooperative precoding and some idealized desired cooperative precoding, subject to the APs' transmit power limits. We note that the precoding deviation is not separable among the APs, and the communication delay between the CC and the APs may span multiple time slots.

- We propose an efficient algorithm, termed Semi-Online Precoding with Information Parsing (SOPIP), to fully account for the heterogeneity in information timeliness and computational capacity in the cooperative network. SOPIP integrates both the timely local CSI and the delayed global CSI to perform precoder updates at both the APs and the CC. In particular, it does not require the CC to send the full global CSI to each AP. Instead, through efficient parsing of the channel and precoder information, SOPIP greatly reduces the amount of communication load on the backhaul. Furthermore, due to its semi-online nature, SOPIP allows adaptive precoder updates at both the CC and the APs through multi-step gradient descent, based on their available computational capacities.

- We analyze the mathematical structure of SOPIP, in the presence of both multi-slot communication delay and gradient estimation error. We show that SOPIP yields $\mathcal{O}(\max\{\tau\Pi_T, \Delta_T\})$ optimality gap in the case of one-step gradient descent at either the CC or the APs, where T is the total time horizon, τ is the round-trip communication delay, Π_T represents the accumulated variation of the desired cooperative precoder in T slots, and Δ_T measures the level of variation in the gradient estimation error in T slots. We further provide an improved performance bound, which shows how the optimality gap decreases as the number of gradient descent steps increases.

- Our simulation results, under typical cellular system settings, show that SOPIP has fast convergence and is tolerant to communication delay. We further demonstrate the performance advantage of SOPIP over other centralized and distributed schemes.

The rest of this paper is organized as follows. In Section II, we present the related work. Section III describes the system model and problem formulation. We present SOPIP and its precoder updates in Section IV. Performance bounds are provided in Section V. Simulation results are presented in Section VI, followed by concluding remarks in Section VII.

II. RELATED WORK

In this section, we survey relevant existing works on cooperative precoding in offline and online scenarios.

1) One-sided Global or Local Cooperative Precoding: Most existing works on cooperative precoding design are based on global processing at the CC (or some equivalent entity). A cooperative zero-forcing (ZF) precoding scheme was studied in [7]. In [8], the impact of synchronization on the cooperative system performance was investigated. Cooperative precoding based on the multi-cell block diagonalization technique was proposed in [9] with per-AP transmit power limits. Compression techniques were used in [10], [11] to reduce the amount of information exchange over the backhaul. In [12], the trade-off between the backhaul cost and power consumption was investigated. Cell-free massive MIMO was proposed in [13], [14], where distributed single-antenna APs are deployed to cooperatively transmit data to the users. The distributed APs rely on the CC for global processing. All of the above works assume the CC has the knowledge of the global CSI without delay, which is restrictive in practical cooperative networks.

Distributed cooperative precoding schemes based only on the local CSI was proposed in [15], [16]. Linear precoding was proposed in [17] for each AP based on the local CSI and the large-scale fading coefficients of the other APs. However, due to the lack of global CSI, the local processing approach may be highly suboptimal.

2) Joint Global and Local Cooperative Precoding: All prior works that adopt the joint global and local processing approach perform one-shot or offline optimization. Cooperative precoding design with AP clustering was considered in [18]. Cooperative transmission in a cognitive network was studied in [19]. An user mobility cooperation approach was proposed in [20] to utilize the moving users for interference mitigation. In [21], the local precoders were optimized through forward and backward training between the CC and APs. Different levels of cooperations between the CC and APs for cell-free massive MIMO was studied in [22]. None of these works considered the impact of backhaul communication delay on the cooperative precoding design over time.

3) Online Convex Optimization for Precoding: The general online convex optimization (OCO) technique [26] accounts for the delayed information in system design. It has been applied to online precoding design problems with delayed CSI in MIMO systems. For example, online projected gradient descent was used in [23] for MIMO uplink precoding design. Dynamic precoding design for point-to-point MIMO systems was studied in [24]. Periodic precoding updates for MIMO network virtualization was considered in [25]. However, these works focused on single-cell MIMO systems and thus cannot be applied to cooperative precoding design.

4) Other Related Works: A part of our proposed algorithm uses the common gradient descent method. However, different from the standard distributed online gradient descent schemes, which assume separable objective functions [27]-[29], our objective function is non-separable among the APs. Therefore, distributed OCO algorithms based only on local information, such as those in [27]-[29], are not applicable to our problem. The need to consider non-ideal backhaul further adds to this challenge.

Decentralized coordinated precoding was considered in [30]-[32], where the APs do not directly cooperate but only

focus on interference mitigation via coordination. In contrast, we focus on the scenario of cooperative communication.

III. SYSTEM MODEL AND PROBLEM FORMULATION

We consider a cooperative wireless MIMO network in a time-slotted system with time index t. As shown in Fig. 1, a total of C APs jointly serve K users with the assistance of a CC over non-ideal backhaul.[1] Each AP c has N^c antennas, so there are $N = \sum_{c=1}^{C} N^c$ antennas in the network. Let $\mathbf{H}_t^c \in \mathbb{C}^{K \times N^c}$ be the local channel state between the K users and AP c. Denote $\mathbf{H}_t = [\mathbf{H}_t^1, \ldots, \mathbf{H}_t^C] \in \mathbb{C}^{K \times N}$ as the global channel state between the K users and all the APs.

At each time slot t, each AP observes the current local CSI $\mathbf{H}_t^c$ and determines its own local precoder $\mathbf{V}_t^c \in \mathbb{C}^{N^c \times K}$ to form cooperative MIMO transmission with the other APs to serve the K users. We impose a maximum transmit power limit $P_{\max}^c$ on $\mathbf{V}_t^c$ via the following local feasible set

$$\mathcal{V}^c \triangleq \{\mathbf{V}^c : \|\mathbf{V}^c\|_F^2 \le P_{\max}^c\} \tag{1}$$

where $\|\cdot\|_F$ denotes the Frobenius norm. Let $\mathbf{V}_t = [\mathbf{V}_t^{1H}, \ldots, \mathbf{V}_t^{CH}]^H \in \mathbb{C}^{N \times K}$ denote the cooperative precoder executed by all the APs at time slot t and $\mathcal{V} = \cup_{c=1}^{C}\{\mathcal{V}^c\}$ be its feasible set. The *actual* received signal vector $\mathbf{y}_t$ (excluding noise) at the K users is given by

$$\mathbf{y}_t = \mathbf{H}_t \mathbf{V}_t \mathbf{x}_t \tag{2}$$

where $\mathbf{x}_t \in \mathbb{C}^{K \times 1}$ is the transmitted signal vector to the K users.[2] Without loss of generality, we assume the signals among users are independent with unit power, *i.e.,* $\mathbb{E}\{\mathbf{x}_t\mathbf{x}_t^H\} = \mathbf{I}, \forall t$.

The APs aim to cooperatively design $\mathbf{V}_t$ to achieve some joint performance objective, *e.g.,* cooperative ZF precoding from all the APs to eliminate inter-user interference and maximize per-user signal gain [7]. However, that would require each AP to have the global CSI, which would be prohibitively expensive to accomplish. Therefore, a common solution is to use a CC to collect the global CSI to centrally design $\mathbf{V}_t$.

Ideally, each AP c communicates $\mathbf{H}_t^c$ to the CC without delay. The CC then has the global CSI $\mathbf{H}_t$ at time slot t and can design a *desired* cooperative precoder $\mathbf{W}_t \in \mathbb{C}^{N \times K}$ in $\mathcal{V}$. Note that the design of $\mathbf{W}_t$ can be based on the service needs of the K users and is *not* limited to any specific precoding scheme. The desired received signal vector (noiseless) $\tilde{\mathbf{y}}_t$ is given by

$$\tilde{\mathbf{y}}_t = \mathbf{H}_t \mathbf{W}_t \mathbf{x}_t. \tag{3}$$

Again, ideally the CC communicates $\mathbf{W}_t$ to the APs without delay, and we have $\mathbf{V}_t = \mathbf{W}_t$ and $\mathbf{y}_t = \tilde{\mathbf{y}}_t$.

---

[1]Alternatively, the AP can represent a base station, a transmission and reception point, or a remote radio unit. The CC can be referred to as central processor, central processing unit, or base-band unit pool.

[2]The signal model in (2) implicitly makes the common assumption that the cooperative network is synchronized in time. There exists over-the-air and broadcasting schemes that can be used to synchronize the clocks at the APs [33], [34]. Also, for cooperative precoding, the user messages are available at the APs.

Fig. 1. An illustration of cooperative MIMO wireless network with non-ideal backhaul communication links.

However, in practice, there is delay in both the uplink and downlink. In this case, the expected deviation of the actual received signal vector at the K users from the desired one is given by $\mathbb{E}\{\|\mathbf{y}_t - \tilde{\mathbf{y}}_t\|_F^2\} = \|\mathbf{H}_t\mathbf{V}_t - \mathbf{H}_t\mathbf{W}_t\|_F^2$. Therefore, we define the precoding deviation of the APs' precoder from the CC's precoder as follows:

$$f_t(\mathbf{V}_t) \triangleq \|\mathbf{H}_t\mathbf{V}_t - \mathbf{H}_t\mathbf{W}_t\|_F^2, \quad \forall t. \tag{4}$$

Note that $f_t(\mathbf{V}_t)$ quantifies the difference between the actual local precoders and the idealized cooperative precoder. Furthermore, $f_t(\mathbf{V}_t)$ is strongly convex in $\mathbf{V}_t$.

A. Problem Formulation

Since the wireless channels dynamically change over time, the goal of our cooperative precoding design is to minimize the accumulated precoding deviation over T time slots, subject to per-AP transmit power limits. The optimization problem is formulated as follows:

$$\textbf{P1:} \quad \min_{\{\mathbf{V}_t \in \mathcal{V}\}_{t=1}^T} \quad \sum_{t=1}^{T} f_t(\mathbf{V}_t).$$

Note that the precoding deviation $f_t(\mathbf{V}_t)$ is *non-separable* among the APs due to the coupling of local channel states $\{\mathbf{H}_t^c\}_{c=1}^C$ and local precoders $\{\mathbf{V}_t^c\}_{c=1}^C$ via inter-AP interference. Therefore, each AP c cannot locally solve **P1** without information exchange with the other APs.

For non-ideal backhaul communication links, at each time slot t, assume the *uplink* delay in sending the timely local CSI $\mathbf{H}_t^c$ from each AP c to the CC is u slots and the *downlink* delay for the CC to send information back to the APs is d slots. We assume the messages to the users are buffered, so that the APs can transmit them at the same time. We consider there is at least one-slot uplink delay, *i.e.,* $u \ge 1$. If the communication overhead is a concern, instead of sending $\mathbf{H}_t^c$, each AP c can send a compressed version of $\mathbf{H}_t^c$, denoted by $\mathbf{L}_t^c$, to the CC.[3] In this case, the CC recovers a delayed global CSI $\hat{\mathbf{H}}_{t-u}$ containing some compression errors.

---

[3]We can readily implement different compression techniques such as those in [10], [11], without major technical changes. Their choice depends on specific requirements on the backhaul and are beyond the scope of this paper.

Since each AP c has its own timely local CSI $\mathbf{H}_t^c$ while the global CSI at the CC is delayed, our optimization setting is *semi-online*. Note that with delayed global CSI, one cannot obtain an optimal solution to **P1**.[4] A widely adopted performance measure in the online optimization literature [35]-[41] is the *dynamic regret* given by

$$\text{RE}_T^{\text{d}} \triangleq \sum_{t=1}^{T} \left(f_t(\mathbf{V}_t) - f_t(\mathbf{V}_t^\star) \right) \tag{5}$$

where $\{\mathbf{V}_t^\star\}_{t=1}^T$ is an offline optimal solution to **P1** assuming the accurate global CSI $\{\mathbf{H}_t\}_{t=1}^T$ is known apriori. In our case, it is clear that $\mathbf{V}_t^\star = \mathbf{W}_t$ for all t, so $\sum_{t=1}^{T} f_t(\mathbf{V}_t^\star) = 0$. Note that minimizing RE_T^{d} is equivalent to solving **P1**.

Remark 1. The globally optimal solution to **P1** is $\mathbf{W}_t$ at each time slot t. However, with non-ideal backhaul, the APs cannot receive $\mathbf{W}_t$ from the CC in time. A naive solution is to directly use the delayed optimal solution $\mathbf{W}_{t-u-d}$ at the APs. In Section VI, we will show that directly using $\mathbf{W}_{t-u-d}$ at the APs leads to inferior performance compared with our proposed algorithm, which utilizes both the more timely local CSI as well as the available computational resource at the APs.

IV. SEMI-ONLINE PRECODING WITH INFORMATION PARSING (SOPIP)

In this section, we present the details of SOPIP. We combine the semi-online setting with the gradient descent approach commonly used in the online optimization literature in order to accommodate the delayed global CSI. However, existing online gradient descent algorithms for distributed networks, *e.g.,* [27]-[29], are not applicable to **P1**, since they implicitly assume the gradient can be computed based only on the local information. For our non-separable global objective function $f_t(\mathbf{V}_t)$ in (4), even discounting the CSI delay, the *current* and *accurate* local gradient at each AP c would be given by

$$\nabla f_t^c(\mathbf{V}_t^c) \triangleq \frac{\partial f_t(\mathbf{V}_t)}{\partial \mathbf{V}_t^{c*}} = \mathbf{H}_t^{cH} \left(\sum_{l=1}^{C} (\mathbf{H}_t^l \mathbf{V}_t^l) - \mathbf{H}_t \mathbf{W}_t \right) \tag{6}$$

where due to inter-AP interference in the received signal, $\nabla f_t^c(\mathbf{V}_t^c)$ depends on its local CSI $\mathbf{H}_t^c$, local precoder $\mathbf{V}_t^c$, and the CSI $\mathbf{H}_t^l$ and precoder $\mathbf{V}_t^l$ at any other AP $l \neq c$. Therefore, to compute its own gradient $\nabla f_t^c(\mathbf{V}_t^c)$, each AP c needs information from the other APs. In SOPIP, we design joint processing algorithms at the APs and the CC to enable local gradient updates at each AP.

Different from existing joint processing approaches, which do not consider the timeliness of CSI or computational capacity at the CC or the APs, SOPIP integrates the timely local and delayed global information to enable precoder updates at both the CC and the APs. Furthermore, the number of precoder updates at both the CC and the APs can be adjustable based on the available computational resource. In the following, we describe the algorithm details of SOPIP at the CC and the APs.

A. CC's Algorithm

In practical cooperative networks, the CC often has a rich amount of computational resource that can be used for cooperative precoder design. At each time slot t, each AP c sends either its accurate or compressed local CSI $\mathbf{L}_t^c$ to the CC. Furthermore, each AP c determines its current local precoder $\mathbf{V}_t^c$ and then sends it together with $\mathbf{L}_t^c$ to the CC. Due to the uplink delay, the CC has the u-slot-delayed local precoder $\mathbf{V}_{t-u}^c$ and CSI $\mathbf{L}_{t-u}^c$ at time slot t. The CC then recovers an approximated version of the local CSI, denoted by $\hat{\mathbf{H}}_{t-u}$, from $\mathbf{L}_{t-u}^c$, which is then used to generate new precoders to assist the local precoder updates at the APs.

Note that the CC needs to accommodate the downlink delay and design the precoders d slots ahead for the APs based on the u-slot-delayed information. To compute the precoder for AP c, the CC initializes an intermediate precoder value $\hat{\mathbf{V}}_{t+d}^{c,0} = \mathbf{V}_{t-u}^c$ for each AP c, and performs J_{CC}-step gradient descent to generate $\hat{\mathbf{V}}_{t+d}^{c,j}, j = 1, \ldots, J_{\text{CC}}$.[5] Due to the uplink delay and CSI compression, the CC only has the *delayed* and *inaccurate* global CSI $\hat{\mathbf{H}}_{t-u}$ and computes the delayed and inaccurate desired cooperative precoder $\hat{\mathbf{W}}_{t-u}$. Given $\hat{\mathbf{H}}_{t-u}$, $\hat{\mathbf{W}}_{t-u}$, and $\hat{\mathbf{V}}_{t+d}^{c,j-1}$, the CC generates an estimate of the local gradient at $\hat{\mathbf{V}}_{t+d}^{c,j-1}$ as

$$\hat{\nabla} f_{t-u}^c(\hat{\mathbf{V}}_{t+d}^{c,j-1}) = \hat{\mathbf{H}}_{t-u}^{cH} \left(\sum_{l=1}^{C} (\hat{\mathbf{H}}_{t-u}^l \hat{\mathbf{V}}_{t+d}^{l,j-1}) - \hat{\mathbf{H}}_{t-u} \hat{\mathbf{W}}_{t-u} \right) \tag{7}$$

for $j = 1, \ldots, J_{\text{CC}}$.

With previous precoder update $\hat{\mathbf{V}}_{t+d}^{c,j-1}$ and gradient estimate in (7), the CC performs the following closed-form projected gradient descent to update $\hat{\mathbf{V}}_{t+d}^{c,j}$:

$$\hat{\mathbf{V}}_{t+d}^{c,j} = \mathcal{P}_{\mathcal{V}^c} \left\{ \hat{\mathbf{V}}_{t+d}^{c,j-1} - \frac{1}{\alpha} \hat{\nabla} f_{t-u}^c(\hat{\mathbf{V}}_{t+d}^{c,j-1}) \right\} \tag{8}$$

where $\alpha > 0$ is a step-size parameter and $\mathcal{P}_{\mathcal{V}^c}\{\mathbf{V}^c\} \triangleq \arg\min_{\mathbf{U}^c \in \mathcal{V}^c}\{\|\mathbf{U}^c - \mathbf{V}^c\|_F^2\}$ is the projection operator onto the local convex feasible set $\mathcal{V}^c$. After the J_{CC}-step gradient descent procedure, to assist the local precoder update at each AP c, the CC then sends $\hat{\mathbf{V}}_{t+d}^{c,J_{\text{CC}}}$ to each AP c.

Furthermore, as an important feature of SOPIP, instead of sending the global CSI to every AP, the CC sends to each AP c the following *parsed* global information on the precoding deviation

$$\hat{\mathbf{G}}_{t-u}^c = \sum_{l=1,l\neq c}^{C} \left(\hat{\mathbf{H}}_{t-u}^l \hat{\mathbf{V}}_{t+d}^{l,J_{\text{CC}}} \right) - \hat{\mathbf{H}}_{t-u} \hat{\mathbf{W}}_{t-u} \in \mathbb{C}^{K \times K}. \tag{9}$$

We summarize the CC's algorithm in Algorithm 1.

Remark 2. Since the global CSI is delayed and possibly inaccurate, in SOPIP, different from the global precoding design approaches, the precoders generated at the CC are not used directly as the final precoders used by the APs. Instead, the CC-generated precoder $\hat{\mathbf{V}}_{t+d}^{c,J_{\text{CC}}}$ along with the parsed global

---

[4]In fact, even for the most basic centralized online problem with one-slot delayed information [35], an optimal solution cannot be found [36].

[5]Later in Sections V and VI, we show that multi-step gradient descent in SOPIP improves the dynamic regret bound and the system performance.

Algorithm 1 SOPIP: CC's algorithm

1: Initialize $\alpha > 0$ and broadcast it all APs.
2: Receive $\mathbf{V}_{t-u}^c$ and $\mathbf{L}_{t-u}^c$ from each AP c.
3: Recover $\hat{\mathbf{H}}_{t-u}^c$ from $\mathbf{L}_{t-u}^c$.
4: Set $\hat{\mathbf{V}}_{t+d}^{c,0} = \mathbf{V}_{t-u}^c$ for each AP c.
5: **for** $j = 1$ **to** J_{CC}
6:     Construct estimated gradient $\hat{\nabla} f_{t-u}^c(\hat{\mathbf{V}}_{t+d}^{c,j-1})$ in (7).
7:     Update $\hat{\mathbf{V}}_{t+d}^{c,j}$ for each AP c via (8).
8: **end for**
9: Send $\hat{\mathbf{V}}_{t+d}^{c,J_{\mathrm{CC}}}$ and $\hat{\mathbf{G}}_{t-u}^c$ to each AP c.

Algorithm 2 SOPIP: AP c's algorithm

1: Initialize $\mathbf{V}_t^c \in \mathcal{V}^c$ at random for any $t \le u$.
2: Receive $\hat{\mathbf{V}}_t^{c,J_{\mathrm{CC}}}$ and $\hat{\mathbf{G}}_{t-u-d}^c$ from the CC.
3: Set $\tilde{\mathbf{V}}_t^{c,0} = \hat{\mathbf{V}}_t^{c,J_{\mathrm{CC}}}$.
4: **for** $j = 1$ **to** J_{AP}
5:     Construct estimated gradient $\hat{\nabla} f_t^c(\tilde{\mathbf{V}}_t^{c,j-1})$ in (10).
6:     Update $\tilde{\mathbf{V}}_t^{c,j}$ via (11).
7: **end for**
8: Set $\mathbf{V}_t^c = \tilde{\mathbf{V}}_t^{c,J_{\mathrm{AP}}}$ and execute $\mathbf{V}_t^c$.
9: Send $\mathbf{V}_t^c$ and $\mathbf{L}_t^c$ to the CC.

information $\hat{\mathbf{G}}_{t-u}^c$ are used at the APs to assist their local precoder updates.

Remark 3. If the CC sends the exact global information $\hat{\mathbf{H}}_{t-u}$, $\hat{\mathbf{V}}_{t+d}^{J_{\mathrm{CC}}}$, and $\hat{\mathbf{W}}_{t-u}$ to each AP c to enable its local precoder updates, the amount of communication overhead is $3NK$. By communicating $\hat{\mathbf{V}}_{t+d}^{c,J_{\mathrm{CC}}}$ and $\hat{\mathbf{G}}_{t-u}^c$ to each AP c, the amount of overhead is $(N^c + K)K$, which is a substantial reduction since we generally have $N \ge K$ in a MIMO network.

Remark 4. Compared with $\hat{\nabla} f_{t-u}^c(\hat{\mathbf{V}}_{t+d}^{c,J_{\mathrm{CC}}})$ in (7), the global information $\hat{\mathbf{G}}_{t-u}^c$ in (9) for AP c does not contain $\hat{\mathbf{H}}_{t-u}^c \hat{\mathbf{V}}_{t+d}^{c,J_{\mathrm{CC}}}$, since more timely local CSI will be used by the AP to reduce the gradient estimation error. Alternatively, instead of sending specific $\hat{\mathbf{G}}_{t-u}^c$ to each AP c, the CC can broadcast the shared global information $\sum_{l=1}^{C}(\hat{\mathbf{H}}_{t-u}^l \hat{\mathbf{V}}_{t+d}^{l,J_{\mathrm{CC}}}) - \hat{\mathbf{H}}_{t-u} \hat{\mathbf{W}}_{t-u} \in \mathbb{C}^{K \times K}$ on the precoding deviation to all the APs. Each AP c can then recover $\hat{\mathbf{G}}_{t-u-d}^c$ locally by subtracting $\hat{\mathbf{H}}_{t-u-d}^c \hat{\mathbf{V}}_t^{c,J_{\mathrm{CC}}}$ at each time slot t, where $\hat{\mathbf{H}}_{t-u-d}^c$ is the previous local CSI that can be recovered from $\mathbf{L}_{t-u-d}^c$ in the same way as the CC.

B. AP c's Algorithm

Recall that each AP c has the current local CSI $\mathbf{H}_t^c$ at time slot t. Since the precoding deviation $f_t(\mathbf{V})$ is non-separable, each AP c cannot compute its local gradient $\nabla f_t^c(\mathbf{V}_t^c)$ in (6) based only on its local CSI. To address this issue, in SOPIP, the CC assists the local gradient estimation by communicating the parsed global information $\hat{\mathbf{G}}_{t-u}^c$ to each AP c. Note that due to the communication delay and CSI compression, the parsed global information is *delayed* and *inaccurate*.

At time slot t, taking into account the additional downlink delay, each AP c receives the parsed global information $\hat{\mathbf{G}}_{t-u-d}^c$ and the intermediate precoder $\hat{\mathbf{V}}_t^{c,J_{\mathrm{CC}}}$ from the CC. Based on $\hat{\mathbf{V}}_t^{c,J_{\mathrm{CC}}}$, each AP c initializes its own intermediate local precoder $\tilde{\mathbf{V}}^{c,0} = \hat{\mathbf{V}}_t^{c,J_{\mathrm{CC}}}$ and performs J_{AP}-step local gradient descent to generate $\tilde{\mathbf{V}}_t^{c,J_{\mathrm{AP}}}$. For each gradient descent step $j = 1, \dots, J_{\mathrm{AP}}$, based on (6), each AP c computes an estimate of the current local gradient at $\tilde{\mathbf{V}}_t^{c,j-1}$ as

$$\hat{\nabla} f_t^c(\tilde{\mathbf{V}}_t^{c,j-1}) = \mathbf{H}_t^{cH}\left(\mathbf{H}_t^c \hat{\mathbf{V}}_t^{c,j-1} + \hat{\mathbf{G}}_{t-u-d}^c\right). \quad (10)$$

Note that the above estimated gradient takes full advantage of the timely local CSI at the AP c, as well as the global information provided by the CC, for the local precoder updates.

Using $\hat{\mathbf{V}}_t^{c,j-1}$ from the previous step and $\hat{\nabla} f_t^c(\tilde{\mathbf{V}}_t^{c,j-1})$ in (10), each AP c performs the following closed-form projected gradient descent to update $\tilde{\mathbf{V}}_t^{c,j}$:

$$\tilde{\mathbf{V}}_t^{c,j} = \mathcal{P}_{\mathcal{V}^c}\left\{\tilde{\mathbf{V}}_t^{c,j-1} - \frac{1}{\alpha}\nabla \hat{f}_t^c(\tilde{\mathbf{V}}_t^{c,j-1})\right\}. \quad (11)$$

Finally, each AP c uses $\mathbf{V}_t^c = \tilde{\mathbf{V}}_t^{c,J_{\mathrm{AP}}}$ as its local precoder for cooperative MIMO transmission with other APs at time slot t. Each AP c then communicates $\mathbf{V}_t^c$ together with the local CSI $\mathbf{L}_t^c$ to the CC. We summarize AP c's algorithm in Algorithm 2.

Remark 5. The computational complexity of the precoder updates in (8) and (11) for each AP c are dominated by matrix multiplications, which are in the order of $\mathcal{O}(NK^2)$ and $\mathcal{O}(N^c K^2)$, respectively. In addition, instead of a total AP transmit power limit, per-antenna transmit power constraints at each AP c can also be incorporated into the local feasible set $\mathcal{V}^c$. In this case, we still have closed-form solutions similar to (8) and (11) with the projection operator now onto the new feasible set $\mathcal{V}_c$.

V. PERFORMANCE BOUNDS

In this section, we present new techniques to derive the performance bounds for SOPIP, to be able to account for the multi-step gradient descent at both the CC and the APs with estimated gradients, in the presence of multi-slot delay.

We first observe that the channel gain is always bounded in practice, *i.e.,* there exists some constant $B > 0$, such that

$$\|\mathbf{H}_t\| \le B, \quad \forall t. \quad (12)$$

In the following lemma, we show that **P1** satisfies several properties that are used in the subsequence analysis: 1) The objective function $f_t(\mathbf{V})$ is strongly convex; 2) $f_t(\mathbf{V})$ is smooth; 3) The impact of the compact convex set $\mathcal{V}$ is bounded; 4) The gradient of the objective function $\nabla f_t(\mathbf{V}) \triangleq \frac{\partial f_t(\mathbf{V})}{\partial \mathbf{V}^*}$ is bounded. The proofs are omitted for brevity.

Lemma 1. Assume the bounded channel gain as in (12). Then, the following statements hold for any $\mathbf{U}, \mathbf{V} \in \mathcal{V}$ and any t:

$$f_t(\mathbf{U}) \ge f_t(\mathbf{V}) + \langle \nabla f_t(\mathbf{V}), \mathbf{U} - \mathbf{V}\rangle_F + \frac{\mu}{2}\|\mathbf{U} - \mathbf{V}\|_F^2, \quad (13)$$

$$f_t(\mathbf{U}) \leq f_t(\mathbf{V}) + \langle \nabla f_t(\mathbf{V}), \mathbf{U} - \mathbf{V} \rangle_F + \frac{L}{2}\|\mathbf{U}-\mathbf{V}\|_F^2, \quad (14)$$

$$\|\mathbf{U}-\mathbf{V}\|_F \leq R, \quad (15)$$

$$\|\nabla f_t(\mathbf{V})\|_F \leq D \quad (16)$$

where $\langle \mathbf{A},\mathbf{B}\rangle_F \triangleq 2\Re\{\mathrm{tr}\{\mathbf{A}^H\mathbf{B}\}\}$, $\mu = 2$, $L = B$, $R = 2\sqrt{\sum_{c=1}^{C} P_{\max}^c}$, and $D = BR$.

We also require the following lemma from [26, Lemma 2.8].

Lemma 2. (Lemma 2.8, [26]) Let $\mathcal{X} \in \mathbb{R}^n$ be a nonempty convex set. Let $h(\mathbf{x}) : \mathbb{R}^n \to \mathbb{R}$ be a ϱ-strongly convex function over $\mathcal{X}$ with respect to a norm $\|\cdot\|$. Let $\mathbf{y} = \arg\min_{\mathbf{x}\in\mathcal{X}}\{h(\mathbf{x})\}$. Then, for any $\mathbf{z} \in \mathcal{X}$, we have $h(\mathbf{y}) \leq h(\mathbf{z}) - \frac{\varrho}{2}\|\mathbf{z}-\mathbf{y}\|^2$.

To proceed with our analysis, we first need to quantify the impact of one-step estimated gradient descent in terms of the gradient estimation error. This is given in the following lemma. Here, for notation simplicity, we denote by $\hat{\nabla}f_t(\mathbf{V})$ a global gradient estimation function with respect to the accurate global gradient $\nabla f_t(\mathbf{V})$, which provides an upper bound on the estimation error for the local gradient estimation schemes in (7) and (10). The proof of this lemma utilizes the results in Lemma 2 and the properties of strong convexity and smoothness while considering the impact of inaccurate gradient. It is omitted due to space limitation.

Lemma 3. Let $\mathbf{U} = \mathcal{P}_\mathcal{V}\{\mathbf{V} - \frac{1}{\alpha}\hat{\nabla}f_t(\mathbf{V})\}$. If we choose $\alpha \geq L$, for any $\gamma \in (0, 2\mu)$, we have

$$\|\mathbf{U}-\mathbf{W}_t\|_F^2 \leq \eta\|\mathbf{V}-\mathbf{W}_t\|_F^2 + \beta\|\nabla f_t(\mathbf{V}) - \hat{\nabla}f_t(\mathbf{V})\|_F^2 \quad (17)$$

where $\eta = \frac{\alpha-\nu}{\alpha+\nu-\gamma} < 1$ and $\beta = \frac{1}{\gamma(\alpha+\nu-\gamma)}$.

Next, we examine the impact of multi-step gradient descent on the dynamic regret bound of SOPIP, in the presence of both gradient estimation error and multi-slot delay. To this end, we need to quantify the accumulated variations of the underlying time-varying system. We define the accumulated variation of the globally optimal solution $\{\mathbf{W}_t\}_{T=1}^{T}$, which is also referred to as the path-length in the OCO literature [35], as $\Pi_T \triangleq \sum_{t=1}^{T}\|\mathbf{W}_t - \mathbf{W}_{t-1}\|_F$. Another important variation measure is the squared path-length, defined as $\Pi_{2,T} \triangleq \sum_{t=1}^{T}\|\mathbf{W}_t - \mathbf{W}_{t-1}\|_F^2$. Note that $\Pi_{2,T}$ is often smaller than Π_T in terms of the growth order [39].[6] Further variation measures are required when we use estimated gradients. To this end, we define the accumulated gradient error as $\Delta_T \triangleq \sum_{t=1}^{T}\max_{\mathbf{V}\in\mathcal{V}}\|\nabla f_t(\mathbf{V}) - \hat{\nabla}f_t(\mathbf{V})\|_F$, and the accumulated squared gradient error as $\Delta_{2,T} \triangleq \sum_{t=1}^{T}\max_{\mathbf{V}\in\mathcal{V}}\|\nabla f_t(\mathbf{V}) - \hat{\nabla}f_t(\mathbf{V})\|_F^2$.

Remark 6. The precoders designed at the CC are based on the information at time slot $t-u$ and arrive at the APs at time slot $t+d$. One can easily verify that only the round-trip delay

[6]For instance $\|\mathbf{W}_t - \mathbf{W}_{t-1}\|_F \propto T^\kappa$ for any t, then $\Pi_T = \mathcal{O}(T^{1+\kappa})$ and $\Pi_{2,T} = \mathcal{O}(T^{1+2\kappa})$. For a sublinear Π_T or $\Pi_{2,T}$, we have $\kappa < 0$ and therefore $\Pi_{2,T}$ is smaller than Π_T in terms of the growth rate. Particularly, if $\kappa = -\frac{1}{2}$, we have $\Pi_{2,T} = \mathcal{O}(1)$ and $\Pi_T = \mathcal{O}(T^{\frac{1}{2}})$.

$u+d$ determines the timeliness of the precoders received at the APs. Therefore, in the following, with out loss of generality, we can equivalently consider the case of τ-slot uplink delay, where $\tau = u + d$, and zero downlink delay.

Based on Lemmas 1-3, for any number of total gradient descent steps $J_{\mathrm{AP}} + J_{\mathrm{CC}} \geq 1$, we provide an upper bound on the dynamic regret RE_T^d of SOPIP in the following theorem.

Theorem 4. For $J_{\mathrm{AP}} + J_{\mathrm{CC}} \geq 1$, if we choose $\alpha \geq L$, the dynamic regret yielded by SOPIP is bounded for any $\gamma \in (0, 2\mu)$ as follows:

$$\mathrm{RE}_T^d \leq 2\tau DR + \frac{2D}{1-\sqrt{\eta^{J_{\mathrm{AP}}+J_{\mathrm{CC}}}}}\left(\tau R + \tau\Pi_T + \frac{2\sqrt{\beta}}{1-\sqrt{\eta}}\Delta_T\right). (18)$$

Proof: We have

$$\mathrm{RE}_T^d = \sum_{t=1}^{T} f_t(\mathbf{V}_t) - f_t(\mathbf{W}_t) \overset{(a)}{\leq} 2\sum_{t=1}^{T}\|\nabla f_t(\mathbf{V}_t)\|_F\|\mathbf{V}_t - \mathbf{W}_t\|_F$$

$$\overset{(b)}{\leq} 2\tau DR + 2D\sum_{t=\tau+1}^{T}\|\mathbf{V}_t - \mathbf{W}_t\|_F \quad (19)$$

where (a) follows from the convexity of $f_t(\mathbf{V})$ and $\langle \mathbf{A},\mathbf{B}\rangle_F \leq 2|\mathrm{tr}\{\mathbf{A}^H\mathbf{B}\}| \leq 2\|\mathbf{A}\|_F\|\mathbf{B}\|_F$, and (b) follows from the feasible set $\mathcal{V}$ and the gradient $\nabla f_t(\mathbf{V})$ being bounded in (15) and (16), respectively.

We now bound the right-hand side (RHS) of (19). We have

$$\sum_{t=\tau+1}^{T}\|\mathbf{V}_t - \mathbf{W}_t\|_F \overset{(a)}{\leq} \sqrt{\eta^{J_{\mathrm{AP}}}}\sum_{t=\tau+1}^{T}\|\hat{\mathbf{V}}_t^{J_{\mathrm{CC}}} - \mathbf{W}_t\|_F + \frac{\sqrt{\beta}\Delta_T}{1-\sqrt{\eta}} \quad (20)$$

where (a) follows from applying Lemma 3 to (11) for J_{AP} times, $\|\mathbf{A}\|_F^2 + \|\mathbf{B}\|_F^2 \leq (\|\mathbf{A}\|_F + \|\mathbf{B}\|_F)^2$ such that $\|\tilde{\mathbf{V}}_t^j - \mathbf{W}_t\|_F \leq \sqrt{\eta}\|\tilde{\mathbf{V}}_t^{j-1} - \mathbf{W}_t\|_F + \sqrt{\beta}\|\nabla f_t(\tilde{\mathbf{V}}_t^{j-1}) - \hat{\nabla}f_t(\tilde{\mathbf{V}}_t^{j-1})\|_F, \forall j = 1,\ldots, J_{\mathrm{AP}}$, and the definition of Δ_T.

We continue to bound the RHS of (20) as follows:

$$\sum_{t=\tau+1}^{T}\|\hat{\mathbf{V}}_t^{J_{\mathrm{CC}}} - \mathbf{W}_t\|_F \overset{(a)}{\leq} \sum_{t=\tau+1}^{T}\|\hat{\mathbf{V}}_t^{J_{\mathrm{CC}}} - \mathbf{W}_{t-\tau}\|_F + \|\mathbf{W}_t - \mathbf{W}_{t-\tau}\|_F$$

$$\overset{(b)}{\leq} \sqrt{\eta^{J_{\mathrm{CC}}}}\sum_{t=\tau+1}^{T}\|\mathbf{V}_{t-\tau} - \mathbf{W}_{t-\tau}\|_F + \frac{\sqrt{\beta}\Delta_T}{1-\sqrt{\eta}} + \tau\Pi_T \quad (21)$$

where (a) is because $\|\mathbf{A}+\mathbf{B}\|_F \leq \|\mathbf{A}\|_F + \|\mathbf{B}\|_F$ and (b) follows from applying Lemma 3 to (8) for J_{CC} times similar to (a) in (20) and the definition of Π_T.

Substituting (21) into (20), and rearranging terms, we have

$$\left(1-\sqrt{\eta^{J_{\mathrm{AP}}+J_{\mathrm{CC}}}}\right)\sum_{t=\tau+1}^{T}\|\mathbf{V}_t - \mathbf{W}_t\|_F - \sqrt{\eta^{J_{\mathrm{AP}}+J_{\mathrm{CC}}}}\sum_{t=1}^{\tau}\|\mathbf{V}_t - \mathbf{W}_t\|_F$$

$$\leq \sqrt{\eta^{J_{\mathrm{AP}}}}\tau\Pi_T + \frac{(\sqrt{\eta^{J_{\mathrm{AP}}}}+1)\sqrt{\beta}}{1-\eta}\Delta_T. \quad (22)$$

Substituting (22) into (21) and noting that $\eta < 1$ and the feasible set $\mathcal{V}$ being bounded in (15), we have (18). ∎

The dynamic regret bound (18) in Theorem 4 improves as the total number of gradient descent steps $J_{\mathrm{AP}} + J_{\mathrm{CC}}$ increases.

When $J_{\text{AP}} + J_{\text{CC}}$ is sufficiently large, we provide another dynamic regret bound for SOPIP below.

Theorem 5. For $J_{\text{AP}} + J_{\text{CC}} > \log_\eta(\frac{1}{2})$, if we choose $\alpha \geq L$, the dynamic regret yielded by SOPIP is bounded for any $\gamma \in (0, 2\mu)$ as follows:

$$\text{RE}_T^{\text{d}} \leq \frac{L}{2(1 - 2\eta^{J_{\text{AP}} + J_{\text{CC}}})} \left(2\tau R^2 + 2\tau^2 \Pi_{2,T} + \frac{3\beta}{1-\eta} \Delta_{2,T} \right). \quad (23)$$

Proof: We have

$$\text{RE}_T^{\text{d}} \overset{(a)}{\leq} \sum_{t=1}^{T} \langle \nabla f_t(\mathbf{W}_t), \mathbf{V}_t - \mathbf{W}_t \rangle_F + \frac{L}{2} \|\mathbf{V}_t - \mathbf{W}_t\|_F^2$$

$$\overset{(b)}{\leq} \frac{L}{2} \tau R^2 + \frac{L}{2} \sum_{t=\tau+1}^{T} \|\mathbf{V}_t - \mathbf{W}_t\|_F^2 \quad (24)$$

where (a) follows from the objective function $f_t(\mathbf{V})$ being L-smooth in (14) and (b) is because $\nabla f_t(\mathbf{W}_t) = \mathbf{0}$ and the feasible set $\mathcal{V}$ is bounded in (15).

We now bound the RHS of (24). We have

$$\sum_{t=\tau+1}^{T} \|\mathbf{V}_t - \mathbf{W}_t\|_F^2 \overset{(a)}{\leq} \sum_{t=\tau+1}^{T} \eta^{J_{\text{AP}}} \|\hat{\mathbf{V}}_t^{J_{\text{CC}}} - \mathbf{W}_t\|_F^2 + \frac{\beta \Delta_{2,T}}{1-\eta} \quad (25)$$

where (a) follows from applying Lemma 3 to (11) for J_{AP} times such that $\|\mathbf{V}_t - \mathbf{W}_t\|_F^2 \leq \eta^{J_{\text{AP}}} \|\hat{\mathbf{V}}_t^{J_{\text{CC}}} - \mathbf{W}_t\|_F^2 + \beta \sum_{i=1}^{J_{\text{AP}}} \eta^{i-1} \|\hat{\nabla} f_t(\tilde{\mathbf{V}}_t^{J_{\text{AP}}-i}) - \nabla f_t(\tilde{\mathbf{V}}_t^{J_{\text{AP}}-i})\|_F^2$ and the definition of $\Delta_{2,T}$.

We continue to bound the RHS of (25) as follows:

$$\sum_{t=\tau+1}^{T} \|\hat{\mathbf{V}}_t^{J_{\text{CC}}} - \mathbf{W}_t\|_F^2 \overset{(a)}{\leq} 2 \sum_{t=\tau+1}^{T} \|\hat{\mathbf{V}}_t^{J_{\text{CC}}} - \mathbf{W}_{t-\tau}\|_F^2 + \|\mathbf{W}_t - \mathbf{W}_{t-\tau}\|_F^2$$

$$\overset{(b)}{\leq} 2 \sum_{t=\tau+1}^{T} \|\hat{\mathbf{V}}_t^{J_{\text{CC}}} - \mathbf{W}_{t-\tau}\|_F^2 + 2\tau^2 \Pi_{2,T}$$

$$\overset{(c)}{\leq} 2 \sum_{t=\tau+1}^{T} \eta^{J_{\text{CC}}} \|\mathbf{V}_{t-\tau} - \mathbf{W}_{t-\tau}\|_F^2 + \frac{2\beta \Delta_{2,T}}{1-\eta} + 2\tau^2 \Pi_{2,T} \quad (26)$$

where (a) is because $\|\mathbf{A} + \mathbf{B}\|_F^2 \leq 2(\|\mathbf{A}\|_F^2 + \|\mathbf{B}\|_F^2)$, (b) follows from $\|\mathbf{W}_t - \mathbf{W}_{t-\tau}\|_F^2 \leq \tau \sum_{i=1}^{\tau} \|\mathbf{W}_{t-\tau+i} - \mathbf{W}_{t-\tau+i-1}\|_F^2$ and the definition of $\Pi_{2,T}$, and (c) follows from applying Lemma 3 to (8) for J_{CC} times similar to (a) in (25).

Substituting (26) into (25) and rearranging terms, we have

$$\left(1 - 2\eta^{J_{\text{AP}} + J_{\text{CC}}} \right) \sum_{t=\tau+1}^{T} \|\mathbf{V}_t - \mathbf{W}_t\|_F^2 - 2\eta^{J_{\text{AP}} + J_{\text{CC}}} \sum_{t=1}^{\tau} \|\mathbf{V}_t - \mathbf{W}_t\|_F^2$$

$$\leq 2\eta^{J_{\text{AP}}} \tau^2 \Pi_{2,T} + \frac{(2\eta^{J_{\text{AP}}} + 1)\beta}{1-\eta} \Delta_{2,T}. \quad (27)$$

Substituting (27) into (24), noting that $\eta < 1$ and the radius of $\mathcal{V}$ being bounded in (15), and on the condition that $2\eta^{J_{\text{AP}} + J_{\text{CC}}} < 1$, we have (23) ∎

From Theorems 4 and 5, we directly conclude the following growth rate of the dynamic regret of SOPIP.

Corollary 6. For $J_{\text{AP}} + J_{\text{CC}} \geq 1$, we have

$$\text{RE}_T^{\text{d}} = \mathcal{O}(\max\{\tau \Pi_T, \Delta_T\}). \quad (28)$$

For $J_{\text{AP}} + J_{\text{CC}} > \log_\eta(\frac{1}{2})$, we have

$$\text{RE}_T^{\text{d}} = \mathcal{O}\left(\min\{\max\{\tau \Pi_T, \Delta_T\}, \max\{\tau^2 \Pi_{2,T}, \Delta_{2,T}\}\} \right). \quad (29)$$

Note that the feedback delay is always bounded by some constant in practice, *i.e.*, $\tau = \mathcal{O}(1)$. Thus, from Corollary 6, a sufficient condition for SOPIP to yield sublinear dynamic regret is either $\max\{\Pi_T, \Delta_T\} = \mathbf{o}(T)$ or $\max\{\Pi_{2,T}, \Delta_{2,T}\} = \mathbf{o}(T)$, *i.e.*, the variation measures grow sublinearly over time. Achieving sublinear dynamic regret is an interesting scenario, since it implies that the time-averaged precoding deviation converges to zero as T goes to infinity.

Remark 7. Sublinearity of the variation measures is necessary to have sublinear dynamic regret for a system with delayed system information [42]. This can be seen from the dynamic regret bounds derived in the OCO literature [35]-[41]. In systems that stabilize over time, leading to sublinear variation measures, we have sublinear dynamic regret.

Remark 8. The semi-online joint global and local gradient descent structure of SOPIP may be viewed as a generalization of several existing studies on generic OCO with strongly convex and smooth objective functions [38]-[40]. All of these works consider only centralized gradient descent, and they are limited to one-slot information delay. With one-step and multi-step gradient descent algorithms, $\mathcal{O}(\Pi_T)$ and $\mathcal{O}(\min\{\Pi_T, \Pi_{2,T}\})$ dynamic regrets were achieved in [38] and [39], respectively, while [40] showed that $\mathcal{O}(\max\{\Pi_T, \Delta_T\})$ dynamic regret can be achieved with one-step gradient descent using inexact gradients. It is easy to see that these regret bounds are special cases of the ones yielded by SOPIP in (28) and (29).

Remark 9. Our proposed algorithm and performance analysis can be extended to accommodate the following concerns in practical systems. 1) If the APs experience different delays, the CC can synchronize the transmissions of the APs based on the maximum delay. 2) If accurate CSI is not available, the APs can use inaccurate CSI instead. It has impact on both the local and global gradient estimation accuracy. 3) When there is local delay, the APs can use the delayed local CSI. Its impact on algorithm performance can be analyzed similarly to the case of delayed global CSI at the CC.

VI. SIMULATION RESULTS

In this section, we present simulation studies under typical cellular system settings. We study the impacts of various system parameters on the convergence and performance of SOPIP. We numerically demonstrate the performance advantage of SOPIP over other centralized and distributed alternatives.

A. Simulation Setup

We consider an urban micro-cell of radius 500 m, with $C = 3$ equally separated APs. Each AP c is equipped with $N^c = 16$ antennas by default. We consider 5 co-located users at the midpoint between every two adjacent APs, for a total of $K = 15$ users in the network by default.

Following the typical cellular system settings [43], we consider transmission over one subcarrier of bandwidth $B_W = 15$
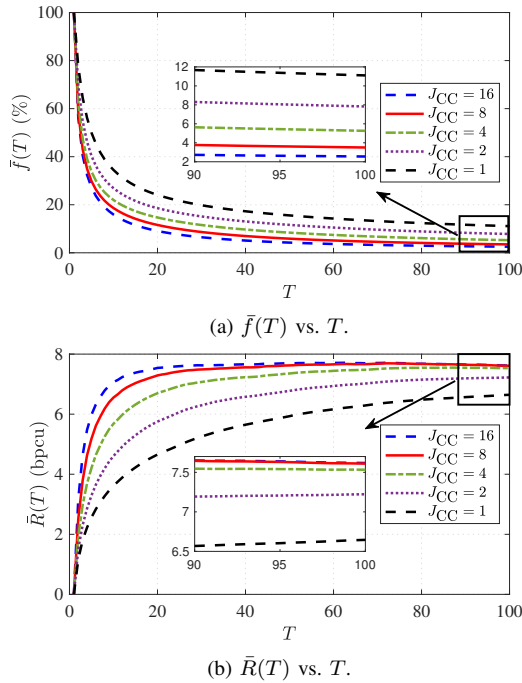
(a) $\bar{f}(T)$ vs. T.

(b) $\bar{R}(T)$ vs. T.

Fig. 2. $\bar{f}(T)$ and $\bar{R}(T)$ vs. T with $J_{\mathrm{AP}} = 1$ and different J_{CC} values.

(a) $\bar{f}(T)$ vs. T.

(b) $\bar{R}(T)$ vs. T.

Fig. 3. $\bar{f}(T)$ and $\bar{R}(T)$ vs. T with $J_{\mathrm{CC}} = 8$ and different J_{AP} values.

kHz and set one time slot to one symbol duration $\frac{1}{B_W} = 66.7$ μs. We set the maximum transmit power limit $P_{\max}^c = 30$ dBm for all c. The receiver thermal noise power spectral density is $N_0 = -174$ dBm/Hz and noise figure is $N_F = 10$ dB. We model the fading channel over time as a first-order Gauss-Markov process [44] $\mathbf{h}_{t+1}^{c,k} = \alpha_{\mathbf{h}} \mathbf{h}_t^{c,k} + \mathbf{z}_t^{c,k}$ between AP c and user k, where $\alpha_{\mathbf{h}} \in [0, 1]$ is the channel correlation coefficient, $\mathbf{h}_t^{c,k} \sim \mathcal{CN}(\mathbf{0}, \beta^{c,k}\mathbf{I})$ with $\beta^{c,k}$ representing the large-scale fading variation consisting of the path-loss and shadowing, and $\mathbf{z}_t^{c,k} \sim \mathcal{CN}(\mathbf{0}, (1 - \alpha_{\mathbf{h}}^2)\beta^{c,k}\mathbf{I})$ is independent of $\mathbf{h}_t^{c,k}$. We model $\beta^{c,k}[\mathrm{dB}] = -31.54 - 33\log_{10}(d^{c,k}) - \psi^{c,k}$ [43], where $d^{c,k}$ is the distance from AP c to user k, and $\psi^{c,k} \sim \mathcal{CN}(0, \sigma_\phi^2)$ is the shadowing effect that is used to model the variation of user positions with $\sigma_\phi^2 = 8$ dB. We set $\alpha_{\mathbf{h}} = 0.998$ as default, which corresponds to user speed 1 km/h. We emphasize here that the Gauss-Markov channel model is used for illustration only. SOPIP can be applied to any arbitrary wireless environment, and neither the CC nor the APs needs to know the channel statistics.

We assume each AP c communicates the exact local CSI $\mathbf{H}_t^c$ to the CC, since the impact of compression error can be emulated by increasing the communication delay τ under the Gauss-Markov channel model. We assume the CC adopts cooperative ZF precoding as its desired cooperative precoder $\mathbf{W}_t^{\mathrm{ZF}} = \sqrt{P_t^{\mathrm{ZF}}}\mathbf{H}_t^H(\mathbf{H}_t\mathbf{H}_t^H)^{-1}$, where $P_t^{\mathrm{ZF}} = \min_{c \in \{1,...,C\}}\{\frac{P_{\max}^c}{\|\mathbf{H}_t^{cH}(\mathbf{H}_t\mathbf{H}_t^H)^{-1}\|_F^2}\}$ maximizes the sum rate subject to per-AP transmit power limits [45].[7]

To measure the performance, we define the time-averaged normalized precoding deviation as $\bar{f}(T) \triangleq$

[7] We assume the K users have the same noise power $\sigma_n^2 = N_F + N_0 B_W$ and therefore all users will have the same rate $\log_2(1 + \frac{P_t^{\mathrm{ZF}}}{\sigma_n^2})$ by using $\mathbf{W}_t^{\mathrm{ZF}}$.
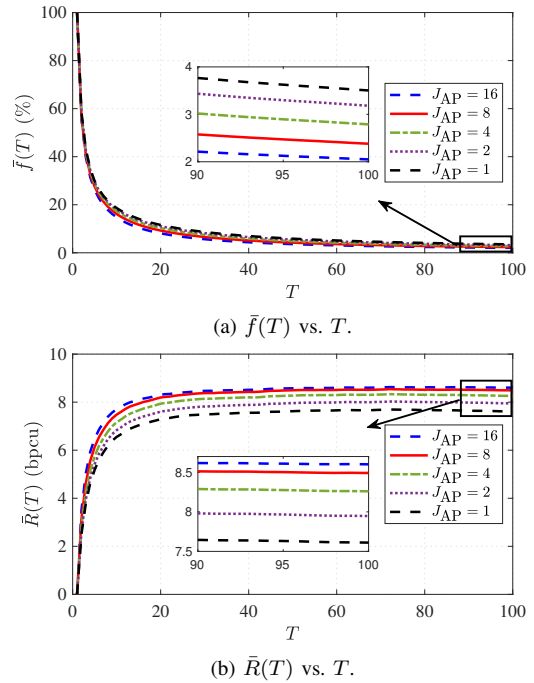
$\frac{1}{T}\sum_{t=1}^{T}\frac{f_t(\mathbf{V}_t)}{\|\mathbf{H}_t\mathbf{W}_t^{\mathrm{ZF}}\|_F^2}$, and the time-averaged per-user rate as $\bar{R}(T) \triangleq \frac{1}{TK}\sum_{t=1}^{T}\sum_{k=1}^{K}\log_2(1 + \mathrm{SINR}_t^k)$, where $\mathrm{SINR}_t^k = \frac{|[\mathbf{H}_t\mathbf{V}_t]_{k,k}|^2}{\sum_{j \neq k}|[\mathbf{H}_t\mathbf{V}_t]_{k,j}|^2 + \sigma_n^2}$ is the signal-to-interference-plus-noise-ratio (SINR) of user k at time slot t with $[\mathbf{A}]_{i,j}$ being the (i, j) element of matrix $\mathbf{A}$.
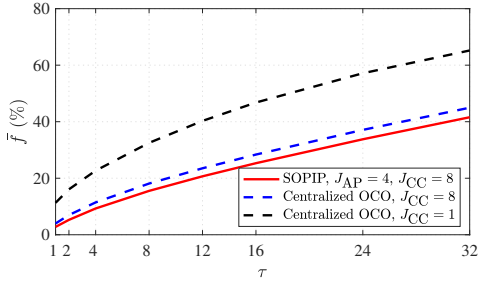
B. Impact of Number of Precoder Update Steps

Fig. 2 and Fig. 3 show $\bar{f}(T)$ and $\bar{R}(T)$ yielded by SOPIP versus T for different numbers of the precoder update steps J_{CC} at the CC and J_{AP} at the APs, respectively. We set the communication delay as one time slot. We observe that SOPIP converges fast (within $T = 100$ time slots). Furthermore, the system performance improves as J_{CC} or J_{AP} increases, showing the performance gain brought by performing multi-step precoder updates with our proposed gradient estimation schemes at either the CC or the APs. As shown in Fig. 2, the system performance almost stabilizes when $J_{\mathrm{CC}} = 8$. Further considering the fact that the APs usually have less computation capacity than the CC, we set $J_{\mathrm{CC}} = 8$ and $J_{\mathrm{AP}} = 4$ as default parameters in the simulation results presented below.
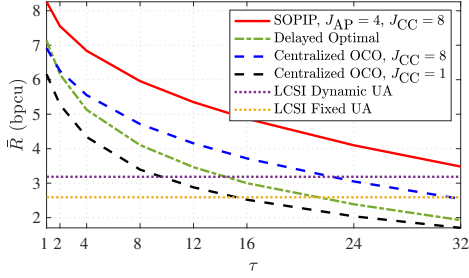
C. Performance Comparison

For comparison, we consider the following schemes.
- *Delayed Optimal:* The CC collects the global CSI from all APs, computes the optimal cooperative precoder, and sends it to all APs. However, due to communication delay, the APs actually execute the delayed precoder $\mathbf{W}_{t-\tau}^{\mathrm{ZF}}$ that can be received from the CC at each time slot t.
- *Centralized OCO:* We run Algorithm 1 at the CC with different numbers of cooperative precoder updates, which can be viewed as the centralized OCO approach. Each AP c executes the precoder $\hat{\mathbf{V}}_t^{c,J_{\mathrm{CC}}}$ (generated based on

(a) $\bar{f}$ vs. τ.

(b) $\bar{R}$ vs. τ.

Fig. 4. Performance comparison on $\bar{f}$ and $\bar{R}$ vs. τ (one time slot is 66.67 μs).

(a) Impact of N^c.

(b) Impact of K.

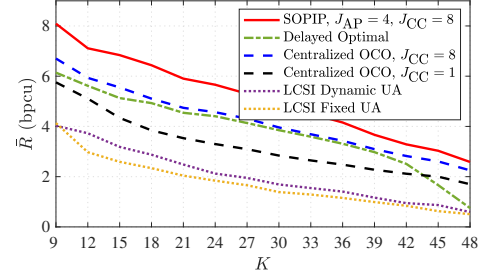Fig. 5. Impacts of N^c and K on $\bar{R}$ with $\tau = 4$.

the delayed global CSI $\mathbf{H}_{t-\tau}$) that can be received from the CC at each time slot t, without performing any local precoder update.

- *Local CSI (LCSIDynamic User Association (UA):* We consider the following distributed precoding scheme. Each user k selects the AP that has the highest channel gain for downlink signal transmission at each time slot t based on the local CSI $\mathbf{H}_t^c$. Let the number of users associated with AP c be K_t^c. Let $\bar{\mathbf{H}}_t^c \in \mathbb{C}^{K_t^c \times N^c}$ denote the available channel state between the K_t^c users and AP c. Each AP c adopts ZF precoding to serve the K_t^c users at each time slot t, given by $\bar{\mathbf{V}}_t^c = \sqrt{\bar{P}_t^c}\bar{\mathbf{H}}_t^{cH}(\bar{\mathbf{H}}_t^c\bar{\mathbf{H}}_t^{cH})^{-1}$, where $\bar{P}_t^c$ is set such that $\|\bar{\mathbf{V}}_t^c\|_F^2 = P_{\max}^c$.

- *LCSI Fixed UA:* This is a more realistic alternative to *LCSI Dynamic UA*. Each user k selects the AP that has the lowest path loss. The user association does not change during our simulation. The APs operate in the same way as under *LCSI Dynamic UA*.

Fig. 4 shows the performance comparison between SOPIP and the alternative schemes of the steady state value of $\bar{f}(T)$ and $\bar{R}(T)$ versus the communication delay τ. Note that $\bar{f}$ is relevant only to SOPIP and *Centralized OCO*. For a wide range of τ values, SOPIP outperforms the distributed alternatives *Dynamic UA* and *Fixed UA*. This demonstrates that even with a large communication delay, utilizing a CC is beneficial to improve the performance. Furthermore, SOPIP outperforms the centralized alternatives *Delay Optimal* and *Centralized OCO*, which demonstrates the importance of performing local precoder updates at the APs. Overall, we observe that, by fully taking advantage of the timely local CSI and delayed global CSI for precoder updates at both the APs and CC, SOPIP substantially outperforms the other centralized or distributed alternatives over a wide range of delay scenarios.
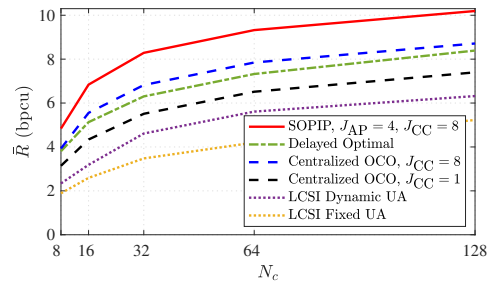
We further study the impacts of the numbers of antennas N^c and users K on the performance of SOPIP with $\tau = 4$. Fig. 5a shows that the steady-state per-user rate $\bar{R}$ increases as the number of antennas N^c increases. This is because the APs have more degrees of freedom to design their cooperative precoding. The steady-state per-user rate $\bar{R}$ dramatically improves as N^c increases, indicating the performance advantage of massive MIMO. Fig. 5b shows that $\bar{R}$ decreases as K increases, due to the increased inter-user interference. We observe that SOPIP substantially outperforms *Delay Optimal* when the number of users is close to the number of antennas. Furthermore, in a wide range of N^c and K values, SOPIP yields the best performance among all alternatives.

VII. CONCLUSIONS

We have studied cooperative precoding design in a MIMO network, where multiple APs jointly transmit signals to serve all the users with the assistance of a CC over non-ideal backhaul. We propose an efficient SOPIP algorithm to minimize the accumulated precoding deviation between the actual and desired cooperative precoders, subject to per-AP transmit power limits. SOPIP allows both timely local precoder updates at the APs and delayed cooperative precoder updates at the CC, by effectively parsing the channel and precoder information. Furthermore, SOPIP allows multi-step precoder updates at both the APs and the CC via gradient descent to fully utilize their available computational resource. Our performance analysis considers the impacts of the multi-step gradient descent at both the CC and the APs, in the presence of both gradient estimation error and multi-slot delay, to derive bounds on the optimality gap. Our simulation results demonstrate the superior delay tolerance and substantial advantage of SOPIP over other centralized and distributed alternatives under a wide rage of scenarios.

REFERENCES

[1] V. Jungnickel, K. Manolakis, W. Zirwas, B. Panzner, V. Braun, M. Los-sow, M. Sternad, R. Apelfrjd, and T. Svensson, "The role of small cells, coordinated multipoint, and massive MIMO in 5G," *IEEE Commun. Mag.*, vol. 52, pp. 44–51, May 2014.

[2] T. L. Marzetta, "Noncooperative cellular wireless with unlimited numbers of base station antennas," *IEEE Trans. Wireless Commun.*, vol. 9, pp. 3590–3600, Nov. 2010.

[3] D. Gesbert, S. Hanly, H. Huang, S. Shamai Shitz, O. Simeone, and W. Yu, "Multi-cell MIMO cooperative networks: A new look at interference," *IEEE J. Sel. Areas Commun.*, vol. 28, pp. 1380–1408, Dec. 2010.

[4] D. Lee, H. Seo, B. Clerckx, E. Hardouin, D. Mazzarese, S. Nagata, and K. Sayana, "Coordinated multipoint transmission and reception in LTE-advanced: deployment scenarios and operational challenges," *IEEE Commun. Mag.*, vol. 50, pp. 148–155, Feb. 2012.

[5] J. Wu, Z. Zhang, Y. Hong, and Y. Wen, "Cloud radio access network (C-RAN): a primer," *IEEE Netw.*, vol. 29, pp. 35–41, Jan. 2015.

[6] J. Zhang, S. Chen, Y. Lin, J. Zheng, B. Ai, and L. Hanzo, "Cell-free massive MIMO: A new next-generation paradigm," *IEEE Access*, vol. 7, pp. 99 878–99 888, Jul. 2019.

[7] O. Somekh, O. Simeone, Y. Bar-Ness, A. M. Haimovich, and S. Shamai, "Cooperative multicell zero-forcing beamforming in cellular downlink channels," *IEEE Trans. Inf. Theory*, vol. 55, pp. 3206–3219, Jul. 2009.

[8] H. Zhang, N. B. Mehta, A. F. Molisch, J. Zhang, and S. H. Dai, "Asynchronous interference mitigation in cooperative base station systems," *IEEE Trans. Wireless Commun.*, vol. 7, no. 1, pp. 155–165, Jan. 2008.

[9] R. Zhang, "Cooperative multi-cell block diagonalization with per-base-station power constraints," *IEEE J. Sel. Areas Commun.*, vol. 28, pp. 1435–1445, Dec. 2010.

[10] S.-H. Park, O. Simeone, O. Sahin, and S. Shamai, "Joint precoding and multivariate backhaul compression for the downlink of cloud radio access networks," *IEEE Trans. Signal Process.*, vol. 61, pp. 5646–5658, Nov. 2013.

[11] B. Dai and W. Yu, "Energy efficiency of downlink transmission strategies for cloud radio access networks," *IEEE J. Sel. Areas Commun.*, vol. 34, pp. 1037–1050, Apr. 2016.

[12] F. Zhuang and V. K. N. Lau, "Backhaul limited asymmetric cooperation for MIMO cellular networks via semidefinite relaxation," *IEEE Trans. Signal Process.*, vol. 62, no. 3, pp. 684–693, Feb. 2014.

[13] H. Q. Ngo, A. Ashikhmin, H. Yang, E. G. Larsson, and T. L. Marzetta, "Cell-free massive MIMO versus small cells," *IEEE Trans. Wireless Commun.*, vol. 16, pp. 1834–1850, Mar. 2017.

[14] E. Nayebi, A. Ashikhmin, T. L. Marzetta, H. Yang, and B. D. Rao, "Precoding and power optimization in cell-free massive MIMO systems," *IEEE Trans. Wireless Commun.*, vol. 16, pp. 4445–4459, Jul. 2017.

[15] R. Zakhour and D. Gesbert, "Distributed multicell-MISO precoding using the layered virtual SINR framework," *IEEE Trans. Wireless Commun.*, vol. 9, pp. 2444–2448, Aug. 2010.

[16] E. Bjrnson, R. Zakhour, D. Gesbert, and B. Ottersten, "Cooperative multicell precoding: Rate region characterization and distributed strategies with instantaneous and statistical CSI," *IEEE Trans. Signal Process.*, vol. 58, pp. 4298–4310, Aug. 2010.

[17] J. Zhang, X. Yuan, and L. Ping, "Hermitian precoding for distributed MIMO systems with individual channel state information," *IEEE J. Sel. Areas Commun.*, vol. 31, pp. 241–250, Feb. 2013.

[18] M. Hong, R. Sun, H. Baligh, and Z.-Q. Luo, "Joint base station clustering and beamformer design for partial coordinated transmission in heterogeneous networks," *IEEE J. Sel. Areas Commun.*, vol. 31, pp. 226–240, 2013.

[19] R. Yao, Y. Liu, L. Lu, G. Y. Li, and A. Maaref, "Cooperative precoding for cognitive transmission in two-tier networks," *IEEE Trans. Commun.*, vol. 64, no. 4, pp. 1423–1436, Apr. 2016.

[20] F. Wang, L. Ruan, and M. Z. Win, "Cooperative network operation design for mobility-aware cloud radio access network," *IEEE Trans. Wireless Commun.*, vol. 17, no. 12, pp. 7819–7833, Dec. 2018.

[21] J. Kaleva, A. Tlli, M. Juntti, R. A. Berry, and M. L. Honig, "Decentralized joint precoding with pilot-aided beamformer estimation," *IEEE Trans. Signal Process.*, vol. 66, pp. 2330–2341, May 2018.

[22] E. Bjrnson and L. Sanguinetti, "Making cell-free massive MIMO competitive with MMSE processing and centralized implementation," *IEEE Trans. Wireless Commun.*, vol. 19, pp. 77–90, Jan. 2020.

[23] P. Mertikopoulos and A. L. Moustakas, "Learning in an uncertain world: MIMO covariance matrix optimization with imperfect feedback," *IEEE Trans. Signal Process.*, vol. 64, pp. 5–18, Jan. 2016.

[24] H. Yu and M. J. Neely, "Dynamic transmit covariance design in MIMO fading systems with unknown channel distributions and inaccurate channel state information," *IEEE Trans. Wireless Commun.*, vol. 16, pp. 3996–4008, Jun. 2017.

[25] J. Wang, B. Liang, M. Dong, and G. Boudreau, "Online MIMO wireless network virtualization over time-varying channels with periodic updates," in *Proc. IEEE Intel. Workshop on Signal Process. Advances in Wireless Commun. (SPAWC)*, 2020.

[26] S. Shalev-Shwartz, "Online learning and online convex optimization," *Found. Trends Mach. Learn.*, vol. 4, pp. 107–194, Feb. 2012.

[27] S. Hosseini, A. Chapman, and M. Mesbahi, "Online distributed optimization via dual averaging," in *Proc. IEEE Conf. Decision Control (CDC)*, 2013.

[28] D. Mateos-Nunez and J. Cortes, "Distributed online convex optimization over jointly connected digraphs," *IEEE Trans. Netw. Sci. Eng.*, vol. 1, pp. 23–37, Oct. 2014.

[29] N. Eshraghi and B. Liang, "Distributed online optimization over a heterogeneous network with any-batch mirror descent," in *Proc. Intel. Conf. Mach. Learn. (ICML)*, 2020.

[30] H. Dahrouj and W. Yu, "Coordinated beamforming for the multicell multi-antenna wireless system," *IEEE Trans. Wireless Commun.*, vol. 9, pp. 1748–1759, May 2010.

[31] L. Venturino, N. Prasad, and X. Wang, "Coordinated linear beamforming in downlink multi-cell wireless networks," *IEEE Trans. Wireless Commun.*, vol. 9, pp. 1451–1461, Apr. 2010.

[32] I. Boukhedimi, A. Kammoun, and M.-S. Alouini, "Coordinated SLNR based precoding in large-scale heterogeneous networks," *IEEE J. Sel. Topics Signal Process.*, vol. 11, pp. 534–548, Apr. 2017.

[33] R. Rogalin, O. Y. Bursalioglu, H. Papadopoulos, G. Caire, A. F. Molisch, A. Michaloliakos, V. Balan, and K. Psounis, "Scalable synchronization and reciprocity calibration for distributed multiuser MIMO," *IEEE Trans. Wireless Commun.*, vol. 13, pp. 1815–1831, Apr. 2014.

[34] O. Abari, H. Rahul, D. Katabi, and M. Pant, "Airshare: Distributed coherent transmission made seamless," in *Proc. IEEE Conf. Comput. Commun. (INFOCOM)*, 2015.

[35] M. Zinkevich, "Online convex programming and generalized infinitesimal gradient ascent," in *Proc. Intel. Conf. Mach. Learn. (ICML)*, 2003.

[36] E. Hazan, A. Agarwal, and S. Kale, "Logarithmic regret algorithms for online convex optimization," *Mach. Learn.*, vol. 69, pp. 169–192, 2007.

[37] A. Jadbabaie, A. Rakhlin, S. Shahrampour, and K. Sridharan, "Online optimization: Competing with dynamic comparators," in *Proc. Intel. Conf. Artif. Intell. Statist. (AISTATS)*, 2015.

[38] A. Mokhtari, S. Shahrampour, A. Jababaie, and A. Ribeiro, "Online optimization in dynamic environments: Improved regret rates for strongly convex problems," in *Proc. IEEE Conf. Decision Control (CDC)*, 2016.

[39] L. Zhang, T. Yang, J. Yi, J. Rong, and Z.-H. Zhou, "Improved dynamic regret for non-degenerate functions," in *Proc. Adv. Neural Info. Proc. Sys. (NIPS)*, 2017.

[40] A. S. Bedi, P. Sarma, and K. Rajawat, "Tracking moving agents via inexact online gradient descent algorithm," *IEEE J. Sel. Topics Signal Process.*, vol. 12, pp. 202–217, 2018.

[41] J. Wang, B. Liang, M. Dong, G. Boudreau, and H. Abou-Zeid, "Delay-tolerant constrained OCO with application to network resource allocation," in *Proc. IEEE Conf. Comput. Commun. (INFOCOM)*, 2021.

[42] O. Besbes, Y. Gur, and A. Zeevi, "Non-stationary stochastic optimization," *Oper. Res.*, vol. 63, pp. 1227–1244, Sep. 2015.

[43] H. Holma and A. Toskala, *WCDMA for UMTS - HSPA evolution and LTE*. John Wiely & Sons, 2010.

[44] I. Abou-Faycal, M. Medard, and U. Madhow, "Binary adaptive coded pilot symbol assisted modulation over rayleigh fading channels without feedback," *IEEE Trans. Commun.*, vol. 53, pp. 1036–1046, Jun. 2005.

[45] K. Karakayali, R. Yates, G. Foschini, and R. Valenzuela, "Optimum zero-forcing beamforming with per-antenna power constraints," in *Proc. IEEE Symposium on Inform. Theory (ISIT)*, 2007.